

Wetting on Lines and Lattices of Cylinders

W. R. Osborn and J. M. Yeomans
Theoretical Physics, 1 Keble Road, Oxford OX1 3NP

May 12, 2018

Abstract

This paper discusses wetting and capillary condensation transitions on a line and a rectangular array of cylinders using an interface potential formalism. For a line of cylinders, there is a capillary condensation transition followed by complete wetting if the cylinders are sufficiently close together. Both transitions disappear as the cylinder separation is increased. The dependence of the wetting phase diagram of a rectangular array of cylinders is discussed as a function of the chemical potential, substrate–fluid interaction strength and surface tension.

PACS: 68.45.Gd and 47.55.Mh

1 Introduction

The wetting of planar surfaces is now well understood [1, 2, 3]. However, in many realistic situations, substrates are far from planar. A particularly important example is provided by porous media, whose wetting properties have implications for fluid flow [4], oil recovery [5] and also the probing of the fractal geometry of surfaces [6]. Our aim in this paper is to describe wetting and capillary condensation on lines and arrays of cylinders as a step towards understanding the properties of binary fluids in complicated geometries.

For such complicated geometries rigorous theoretical methods quickly become intractable and approximations must be made. A profitable approach has been to use an interface potential which replaces the density profile at a fluid–fluid interface by a sharp kink and uses a local surface tension [1, 3]. This approach is valid far from the bulk critical point and for wetting layers thicker than a few intermolecular spacings. It has the advantage that it is easily implemented, yet provides qualitatively correct phase diagrams.

Cheng and Cole [7] and Napiórkowski et al. [8] applied the interface potential approach to wetting in a corner, Darbellay and Yeomans [9] to wetting in a slit, and Robbins et al. [10] to wetting on a line of slits. Dobbs et al. [11] extended the approach to treat two spheres, and subsequently a square array of cylinders [12] in both the grand canonical and the more physically realistic canonical ensembles. In each case, sensible qualitative results were obtained for the phase behaviour although, as one might expect, subtle details of the interface position are not given correctly [3].

In Section 2 we use such an interface potential approach to study wetting on a line of cylinders. We consider the case of Van der Waals interparticle interactions. If the cylinders are close enough together for a capillary condensation transition to occur, the system undergoes complete wetting as $\tilde{\Delta\mu} \rightarrow 0$. Otherwise, the cylinders behave individually rather than collectively and the wetting transition is suppressed.

In Section 3, a rectangular array of cylinders is considered. The phase diagram is determined as a function of the aspect ratio of the array, the chemical potential, the strength of the Van der Waals interactions, and the surface tension. Limiting cases in which this substrate reverts to the line of cylinders described in Section 2 and the square array considered by Dobbs and Yeomans [12] are discussed.

Although using the interface potential approach significantly simplifies the problem, it is still not easy to study the more complicated geometries which will model a porous medium more closely. For example, even for an array of spherical substrates, the non-linear differential equations that must be solved become two- rather than one-dimensional. Therefore, in Section 4, we describe a simpler way of modelling the different phases, which is amenable to extension to more complicated regular and random geometries. A comparison to the solutions of the interface potential ap-

proach allows us to assess its usefulness.

Our results are summarised in Section 5.

2 An Infinite Line of Cylinders

Firstly, we consider wetting on an infinite line of identical cylinders lying along the x -axis with their axes parallel to the z -axis, as shown in Figure 1. The cylinders have radius r_0 and their separation is L' . The relevant part of the grand potential per cylinder, per unit length in the z -direction, is taken to be

$$\Phi = 4 \left(\int_0^{+L'/2} \left\{ \sigma \sqrt{1 + l_x^2(x)} + \widetilde{\Delta\mu} \left(l(x) - \frac{\pi r_0^2}{2L'} \right) \right\} dx + W[l(x)] \right) \quad (1)$$

where $l(x)$ is the interface position and the subscript x denotes differentiation with respect to x .

The first term in equation (1) is the free energy of the liquid–gas interface, the surface tension σ multiplied by the surface area. The second is a bulk term due to the excess cost of the adsorbed, unfavourable liquid. If ρ_l and ρ_g are the liquid and gas number densities, respectively, then the free energy per unit volume of the liquid phase over and above that of the gas phase is

$$\widetilde{\Delta\mu} = (\mu_c - \mu^*)(\rho_l - \rho_g) \quad (2)$$

with μ^* the chemical potential of the fluid in the system and μ_c the chemical potential at bulk liquid–gas coexistence.

The final term models the interparticle interactions which, for non-retarded Van-der-Waals forces, can be written

$$W[l(x)] = \int_0^{+L'/2} \int_{l(x)}^{\infty} \Pi[x', y(x'), r_0, L'] dy dx' \quad (3)$$

with a disjoining pressure

$$\Pi(x, y, r_0, L') = \sum_i \int_{\text{cylinder } i} \frac{W'_0}{|r - \underline{r}'|^6} d\underline{r}' \quad (4)$$

where the summation is taken over all cylinders i . Note that the integrals in equations (3) and (4) are over the gas and substrate; all other interactions are either independent of $l(x)$ or can be reformulated as integrals over these regions. The strength of the interactions is $W'_0 = A/\pi^2$ where A is the conventionally defined Hamaker constant.

The integral in equation (4) cannot be performed analytically, in contrast to the cases of a spherical substrate [13] and a cylindrical pore [14], but the numerical result is well fit by a function

$$\Pi[x, y, r_0, L'] \approx W'_0 \sum_{i=-\infty}^{\infty} \left(\frac{\pi e^{-(l_i/r_0-1)}}{6(l_i-r_0)^3} + \frac{3\pi^2 r_0^2}{8l_i^5} \right) \quad (5)$$

where l_i is the distance from the centre of cylinder i to the point \underline{r} . The first term in the expression (5) is accurate at small distances from a cylinder, when the substrate acts like a flat plane. The second gives the correct behaviour in the long distance limit. The fit (5) agrees with numerical integration of the disjoining pressure to within 10%, with the largest discrepancy occurring in the crossover region, at a distance of about r_0 from the surface of a cylinder. This discrepancy is unimportant because the contribution of the interactions to the total free energy is small compared to that of the surface energy at this distance.

The grand free energy, Φ , can be minimised with respect to $l(x)$ using the Euler-Lagrange formula, yielding a non-linear differential equation

$$\frac{d}{dx} \left(\frac{\sigma l_x}{\sqrt{(1+l_x^2)}} \right) - \widetilde{\Delta\mu} + \Pi[x, l(x), r_0, L'] = 0 \quad (6)$$

A solution where the liquid forms bridges between the cylinders (see Figure 1) may be found if this is solved with boundary conditions $l_x = 0$ at $x = 0$ and $x = L'/2$.

To find the unbridged solution, where the interface wraps around each individual cylinder, it is necessary to formulate the problem in polar coordinates with the origin at the centre of a cylinder. The Euler-Lagrange minimisation then gives

$$\frac{d}{d\theta} \left(\frac{\sigma l_\theta}{\sqrt{(l^2 + l_\theta^2)}} \right) - \widetilde{\Delta\mu} l(\theta) + \Pi[\theta, l(\theta), r_0, L'] l(\theta) - \frac{\sigma l(\theta)}{\sqrt{(l^2 + l_\theta^2)}} = 0 \quad (7)$$

The boundary conditions are $l_\theta = 0$ at $\theta = 0$ and $\theta = \pi/2$, where $l_\theta \equiv dl(\theta)/d\theta$.

The solutions to the differential equations (6) and (7) can be found numerically using a relaxation method for different values of the parameters $\mu = \widetilde{\Delta\mu} r_0 / \sigma$, $L = L'/r_0$ and $W_0 = W'_0 / (\sigma r_0^2)$. Once the interface profiles are known, the grand free energy of each phase can be calculated from equation (1) using numerical integration techniques, allowing comparison of the free energies and determination of the stable configuration.

The resulting phase diagram is shown in Figure 2. For $L < 2$ the cylinders are overlapping and the problem is not defined. The unbridged phase is stable at large μ , as expected. For $2 < L < L_c(W_0)$, as μ is decreased there is a first-order phase transition to the bridged phase and then, as $\mu \rightarrow 0$ the interface unbonds to infinity, an example of a complete wetting transition. As the surface unbonds to large distances, it becomes flat and it follows from (5) and (6) that

$$\widetilde{\Delta\mu} \sim \frac{\pi^2 r_0^2 W_0'}{2 L' l^4} \text{ as } l \rightarrow \infty \quad (8)$$

This shows that the line of cylinders is behaving, as expected, like a plate of effective thickness $\pi r_0^2 / L'$.

For $L > L_c$, capillary condensation does not occur as μ decreases and the complete wetting transition is suppressed by the substrate geometry. For vanishingly small W_0 at $\mu = 0$, the surface area is the only relevant quantity. The liquid–gas surface area per unit length for a single cylinder in the unbridged phase is $2\pi r_0$ while that of a bridged film is $2L_c r_0$, giving $L_c(0) = \pi$ in agreement with the numerical solution.

As W_0 is increased at fixed μ , the interfaces lie further from the substrates. For an approximately flat, bridged interface the surface energy is virtually unchanged by this. However, for the unbridged solution the surface area and hence the surface energy must increase as the interface moves. Thus the unbridged solution becomes less favourable for a given μ , as seen in Figure 2.

3 An Infinite Rectangular Array of Cylinders

An infinite number of lines of cylinders can be brought together to produce a rectangular array with inter-line distance D' , as shown in Figure 3. As $D = D'/r_0$ is reduced, this system shows a crossover from the behaviour of a line of cylinders to that reported in Dobbs and Yeomans [12] for a square array.

Two new phases might be expected to exist. The first of these consists of bridging between lines of cylinders as well as between the cylinders in one line. To find such a doubly-bridged solution it is necessary to use a polar coordinate system centred on an interstitial site such as point A in Figure 3. The Euler-Lagrange minimisation then gives

$$\frac{d}{d\theta} \left(\frac{\sigma l_\theta}{\sqrt{(l^2 + l_\theta^2)}} \right) + \widetilde{\Delta\mu} l(\theta) - \Pi [l', l(\theta'), r_0, L'] l(\theta) - \frac{\sigma l(\theta)}{\sqrt{l^2 + l_\theta^2}} = 0 \quad (9)$$

where l' and θ' are the distance and angle to point (l, θ) from the centre of one of the four nearest cylinders. The boundary conditions are that $l_\theta = 0$ at $\theta = 0$ and $\theta = \pi/2$. Equation (9) is solved numerically, as before.

There is also a phase where the space between the cylinders is completely filled with liquid. The free energy of this per cylinder, per unit length in the z -direction is

$$\Phi_{\text{full}} = \widetilde{\Delta\mu} (L' D' - \pi r_0^2) \quad (10)$$

From comparisons of the free energies, the stable configuration can be found for given values of the four parameters $L, D, \mu = \widetilde{\Delta\mu} r_0 / \sigma$ and

$W_0 = W'_0/\sigma r_0^2$. Typical values of the Hamaker constant for a condensed phase are of order $(0.4-4) \times 10^{-19}$ J, while typical interfacial energies lie in the range $(2-8) \times 10^{-2}$ J m⁻² [15]. If we suppose that the cylinders are of the same size as the grains in a porous rock, then $r_0 \sim (1-100) \times 10^{-6}$ m, giving $W_0 \sim 10^{-6}$.

Phase diagrams are plotted in Figures 4 and 5 and are discussed below.

- Small L

Figure 4 shows a cross-section through the phase diagram for $L = 2.2$ and $W_0 = 2.5 \times 10^{-6}$. For any finite D , the behaviour is no longer that of many separate horizontal lines of cylinders. Complete wetting at $\mu = 0$ is replaced by a transition to a full phase at $\mu > 0$. For large D , this transition lies along the line $D = 2/\mu$. As D decreases, the phase which is singly-bridged along the \hat{x} -direction becomes unstable, as expected, and the doubly-bridged solution is favoured. For $D = L = 2.2$, symmetry demands that singly-bridged solutions cannot be stable and we recover, as expected, a phase diagram topologically similar to that of Dobbs and Yeomans for a square array [12].

For $D < L$, as μ is decreased the system jumps from being unbridged to singly-bridged along \hat{y} to doubly-bridged to full, the order of increasing liquid volume.

- Increasing L

For $L = 2.6$, $W_0 = 2.5 \times 10^{-6}$, the phase diagram is that shown in Figure 5. As L is increased, the quadruple point B in Figure 4 moves to lower values of μ until it coincides with point A , when the doubly-bridged phase disappears from the phase diagram. Moreover, the phase which is singly-bridged along \hat{x} is stable only at increasingly high values of D as L is increased further until $L \equiv L_c^*$, when it becomes thermodynamically unstable for all D . L_c^* is, as expected, approximately equal to L_c , the critical value above which a line of cylinders does not undergo complete wetting, with small corrections due to the influence of the other cylinders in the array.

- Increasing W_0

When W_0 is increased, at a given value of μ the free energy of phases with more interface close to a surface will increase relatively more than those with less. Hence the transition lines move to greater values of μ . For $W_0 = 2.5 \times 10^{-5}$ and $L = 2.2$, the phase diagram is like that in Figure 4 but point B moves to $\mu \approx 6.67$ while point A moves to values of μ and D greater by $\sim 3\%$.

4 Simple Model

The interface potential approach already involves considerable approximation. However, it still relies on the high symmetry of the system considered to produce tractable, one-dimensional, non-linear differential

equations. To better model porous media it would be desirable to be able to treat more complicated substrate geometries. Thus, we now consider a much simpler way of modelling the phases in the cylindrical array and compare the resulting phase diagrams with those obtained from the interface potential approach. We find only small discrepancies for physically realistic W_0 , giving confidence that the simpler model will give qualitatively correct phase diagrams for more realistic models of porous media.

The approach is to approximate the interface shapes in the different thermodynamically stable phases by simple curves that can be handled analytically. The effect of the Van der Waals interaction is incorporated by assuming that where an interface wraps around a cylinder it lies a distance r from the centre of the cylinder, where r follows from the flat plane result

$$r - r_0 = \sqrt[3]{\frac{W'_0 \pi}{6 \Delta \mu}} \quad (11)$$

Where the liquid forms bridges between cylinders, the bridges are taken to have a radius of curvature $a = \sigma/\Delta\mu \equiv r_0/\mu$, which follows from minimising the free energy of a bridge with respect to a . By assuming that the arcs of radius r and a meet tangentially, the interface shape is completely defined.

The different phases can be modelled as shown in Figure 6.

- Unbridged phase
A circle of radius r , centred on a cylinder.
- Singly-bridged phase
An arc of radius r , centred on a cylinder, for $\theta > \theta_0$, with θ measured from the direction of bridging. An arc of radius a tangential to this at $\theta = \theta_0$, with $\frac{\partial l}{\partial x} = 0$ at $x = L'/2$, where $\cos \theta_0 = \frac{L'}{2(r+a)}$.
- Doubly-bridged phase
An arc of radius r , centred on a cylinder, for $\theta_0 < \theta < \theta_1$. Two arcs of radius a tangential to this, the first at $\theta = \theta_0$ with $\frac{\partial l}{\partial x} = 0$ at $x = L'/2$, where $\cos \theta_0 = \frac{L'}{2(r+a)}$ and the second at $\theta = \theta_1$ with $\frac{\partial l}{\partial y} = 0$ at $y = D'/2$, where $\cos \theta_1 = \frac{D'}{2(r+a)}$.

The grand free energy is taken to be

$$\Phi = \sigma \times \text{interface area} + \widetilde{\Delta \mu} \times \text{fluid volume} \quad (12)$$

The stable state can be determined by comparing the free energy of the different phases. Despite the simplicity of the approach the phase diagrams in Figures 4 and 5 are reproduced to within 1%.

Note that a term representing the interaction energy has not been included explicitly in equation (12). It can be estimated by, for example, considering only those parts of an interface which adhere to the substrate as making a contribution. However, for the unbridged solution the ratio of the surface free energy to the interaction or volume terms $\sim \sqrt[3]{W_0}$. For a

bridged phase the volume component of the free energy increases, but the contribution from the interactions remains of the same order of magnitude. Therefore, for the values of W_0 considered here, the contribution of the interactions to the total free energy $\sim 1\%$ and can reasonably be neglected given the level of approximation already inherent in the approach.

5 Discussion

In this paper we have described wetting on a line and rectangular array of cylinders. For a line of cylinders a capillary condensation or bridging transition is followed by complete wetting as $\mu \rightarrow 0$. If the cylinders are sufficiently far apart bridging does not occur and the wetting transition is suppressed: the cylinders are now behaving individually rather than as an effectively planar substrate.

For an array of cylinders we have calculated the phase diagram as a function of the aspect ratio and reduced chemical potential. Several different capillary condensation transitions occur: to states bridged in the \hat{x} or \hat{y} directions; to a doubly-bridged phase or to a phase where the liquid completely fills the volume between the cylinders.

The thin–thick transitions which correspond to wetting on a cylindrical substrate [13, 16] are not included in this model where we consider an effective interface potential with a single minimum. The results of Dobbs and Yeomans [17] for adjacent spheres indicate that including retarded Van der Waals terms in the potential to model such transitions would not substantially affect capillary condensation, while the thin–thick transition lines would essentially follow those for an individual cylinder.

The phase diagrams have been obtained using an interfacial potential approximation which treats the interface as a sharp delineation between the two phases. The interface position is obtained as the solution of a non-linear differential equation. The feasibility of the approach is dependent on the high symmetry of the system we have considered. To better model porous media it is important to be able to treat more complicated substrates. Therefore we have tested a simpler approach where the shape of the interface in each phase is fed in as an assumption. The results agree very well with those obtained by the interface potential method giving us confidence that the simple approach will give realistic results for substates approximating more closely those found in porous media.

There have been micromodel experiments undertaken on regular two-dimensional arrays [18] where capillary condensation is seen to play a role in the flow of a binary liquid mixture through the model porous medium. Our results apply to static configurations of the liquid but may supply insight into the flow properties.

Acknowledgements

It is a pleasure to thank H. T. Dobbs and J. O. Indekeu for many useful discussions. WRO acknowledges support from a SERC CASE studentship with British Gas plc, and JMY from a SERC Advanced Fellowship.

References

- [1] M. Schick in *Liquids at Interfaces (Les Houches Session XLVIII)*. J. Charvolin, J. F. Joanny, and J. Zinn-Justin, editors. North Holland, Amsterdam, (1990).
- [2] D. E. Sullivan and M. M. Telo de Gamma in *Fluid Interfacial Phenomena*. C. A. Croxton, editor. Wiley, New York, (1986).
- [3] S. Dietrich in *Phase Transitions and Critical Phenomena*. C. Domb and J. Lebowitz, editors, volume 12. Academic Press, London, (1988).
- [4] D. Wilkinson in *Mathematics in Oil Production*. S. Edwards and P. R. King, editors. Clarendon Press, Oxford, (1988).
- [5] E. J. Hinch in *Mathematics in Oil Production*. S. Edwards and P. R. King, editors. Clarendon Press, Oxford, (1988).
- [6] P. Pfeifer and M. W. Cole. *New Journal of Chemistry*, **14**, 221, (1990).
- [7] E. Cheng and M. W. Cole. *Phys. Rev. B* **41**, 9650, (1990).
- [8] M. Napiórkowski, W. Koch, and S. Dietrich. *Phys. Rev. A* **45**, 5760, (1992).
- [9] G. A. Darbellay and J. M. Yeomans. *J. Phys. A* **25**, 4275, (1992).
- [10] M. O. Robbins, D. Andelman, and J. F. Joanny. *Phys. Rev. A* **43**, 4344, (1991).
- [11] H. T. Dobbs, G. A. Darbellay, and J. M. Yeomans. *Europhys. Lett.* **18**, 439, (1992).
- [12] H.T. Dobbs and J. M. Yeomans. *Molecular Physics* (to appear), (1993).
- [13] M. P. Gelfand and R. Lipowsky. *Phys. Rev. B* **36**, 8725, (1987).
- [14] M. W. Cole and W. F. Saam. *Phys. Rev. Lett.* **32**, 985, (1974).
- [15] J. N. Israelachvili. *Intermolecular and Surface Forces, 2nd edition*. Academic Press, London, (1992).
- [16] P. J. Upton, J. O. Indekeu, and J. M. Yeomans. *Phys. Rev. B* **40**, 666, (1989).
- [17] H. T. Dobbs and J. M. Yeomans. *J. Phys. : Condensed Matter* **4**, 10133, (1992).
- [18] A. Danesh, D. Krinis, G. D. Henderson, and J. M. Peden. *J. Petroleum Sci. and Eng.* **2**, 167, (1989).

Figure Captions

Figure 1 The arrangement of fluid around a line of cylinders for a bridged phase.

Figure 2 Dependence of the bridging transition of a single line of cylinders on the reduced Van der Waals interaction W_0 : solid line, $W_0 = 0$; long-dashed line, $W_0 = 2.5 \times 10^{-6}$; shorter-dashed line, $W_0 = 2.5 \times 10^{-4}$.

Figure 3 Part of a rectangular array of cylinders, showing the doubly-bridged phase.

Figure 4 The phase diagram of an array of cylinders with $L = 2.2$ and $W_0 = 2.5 \times 10^{-6}$.

Figure 5 The phase diagram of an array of cylinders with $L = 2.6$ and $W_0 = 2.5 \times 10^{-6}$.

Figure 6 The approximate geometries used to model the interface position in the approach described in §4 : (i) unbridged phase, (ii) bridged phase, (iii) doubly-bridged phase. $a = r_0/\mu$.

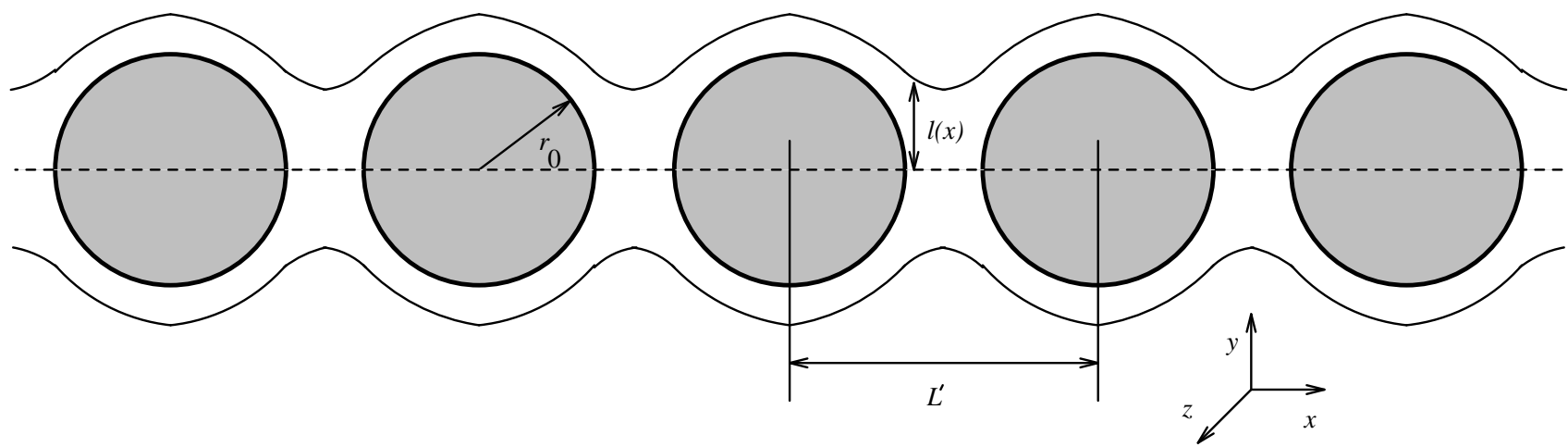


Figure 1

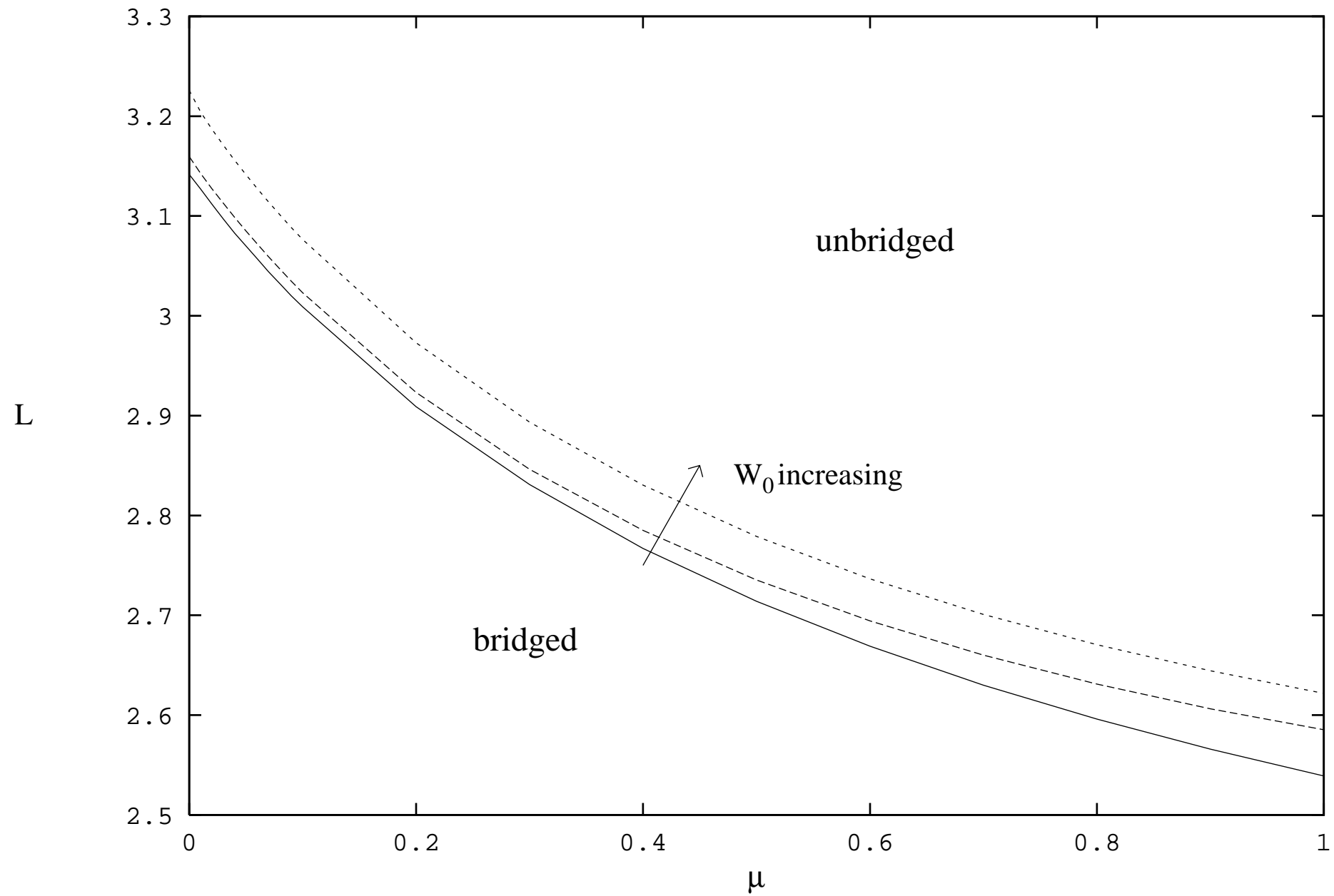


Figure 2

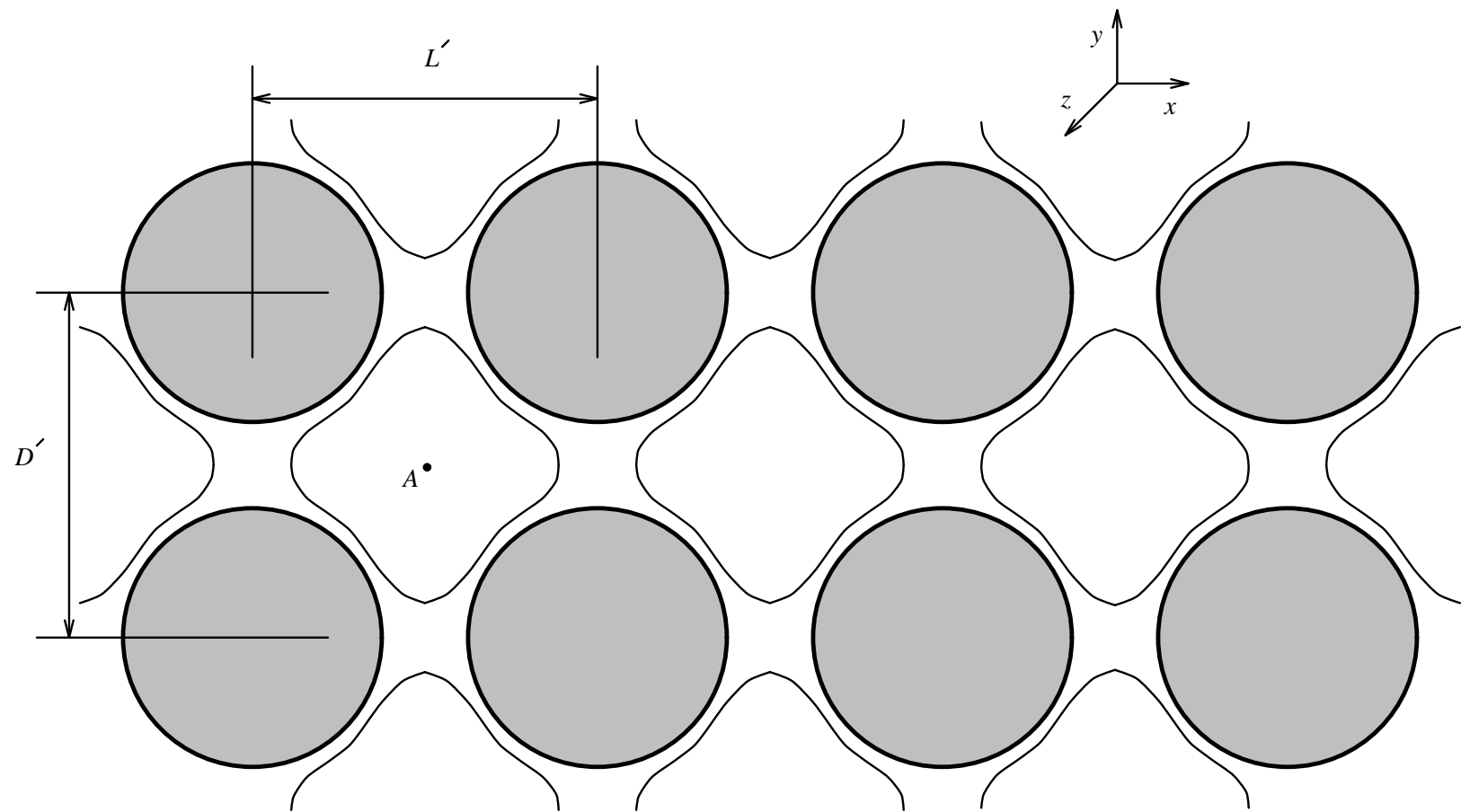


Figure 3

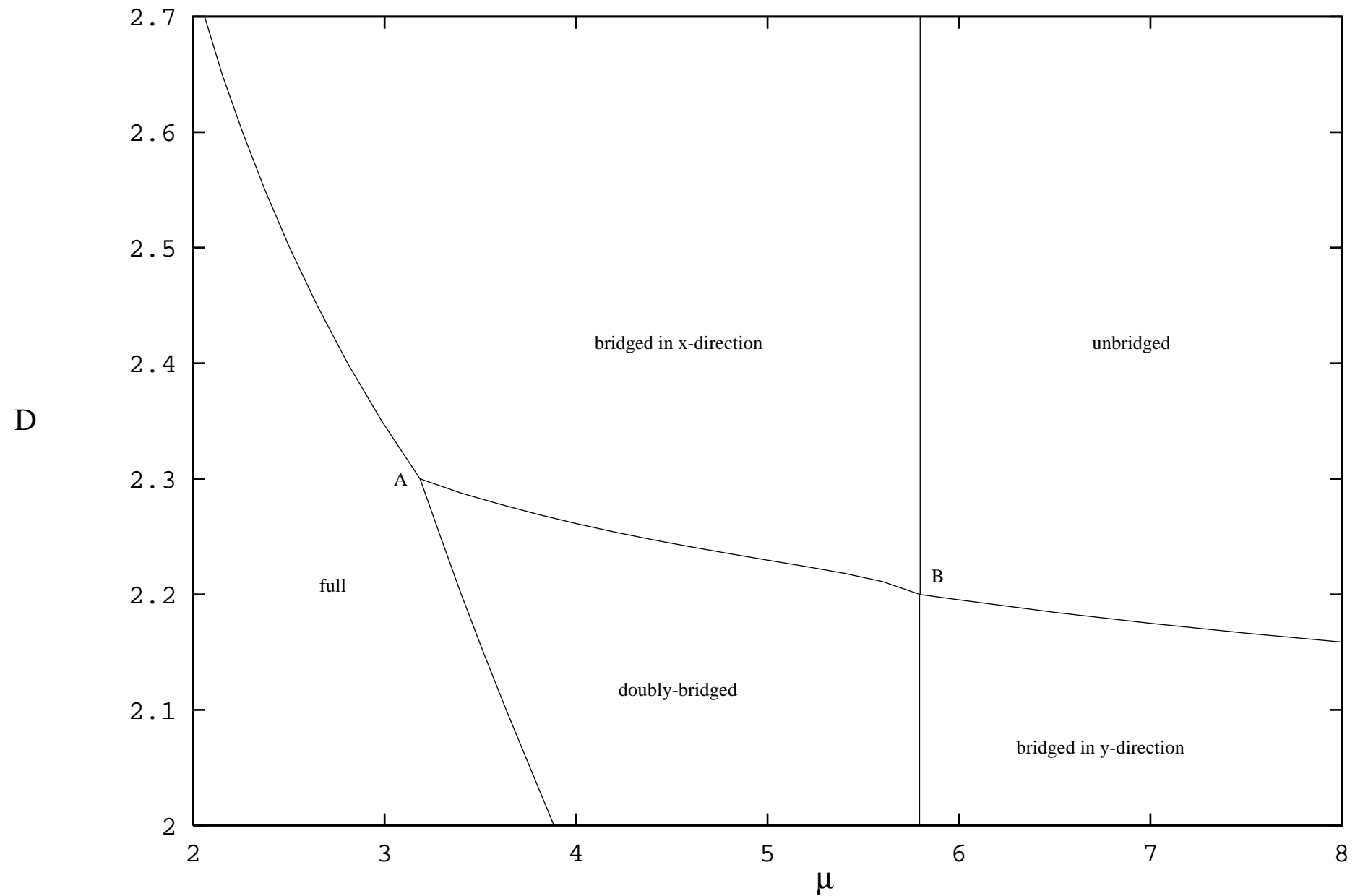


Figure 4

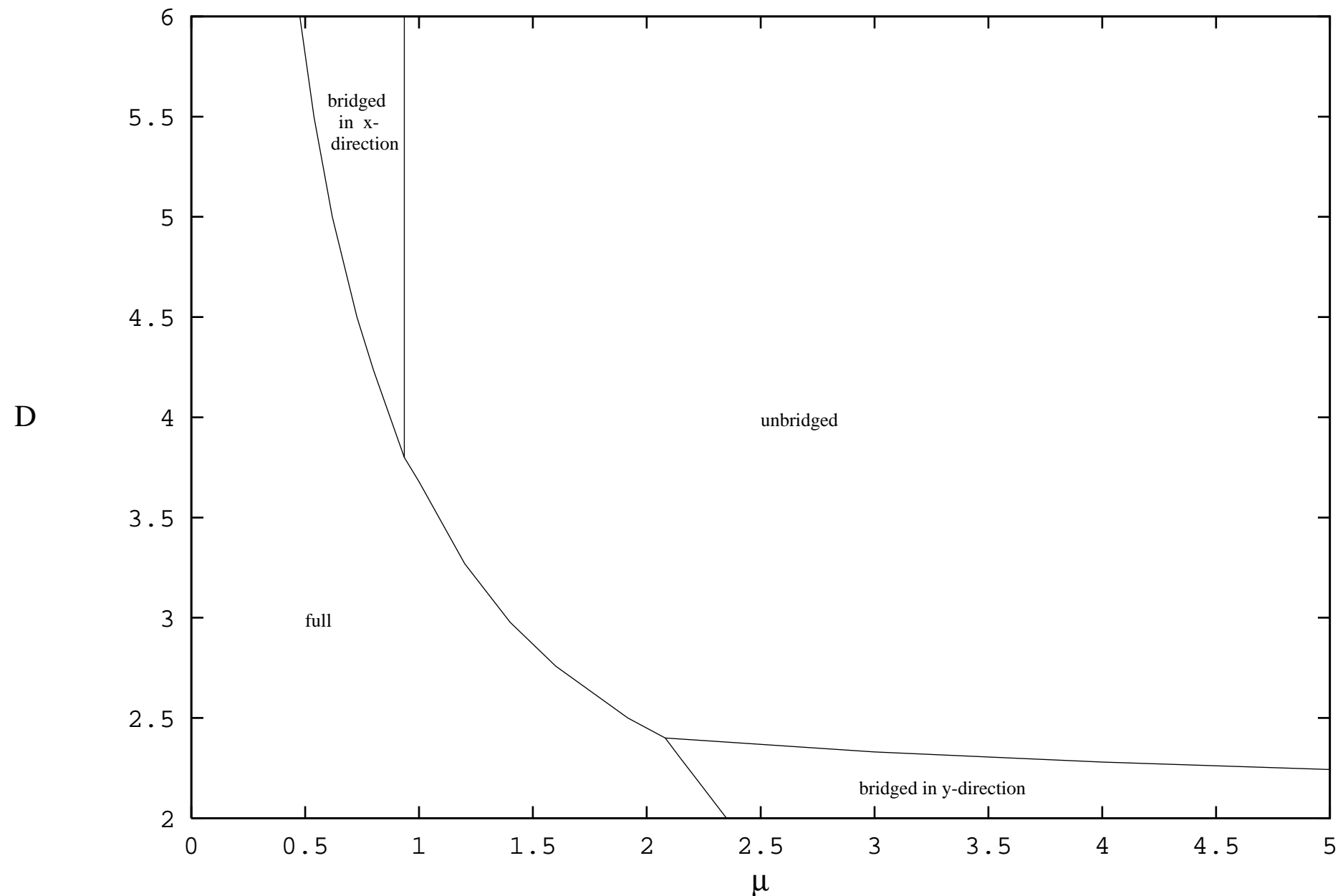
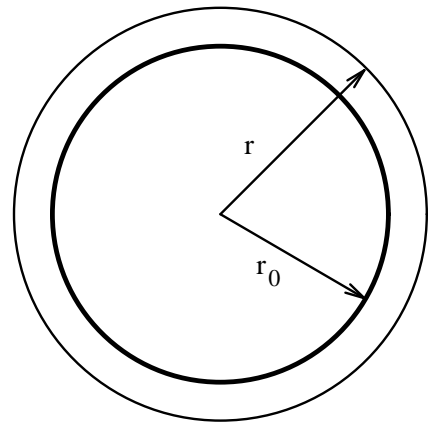
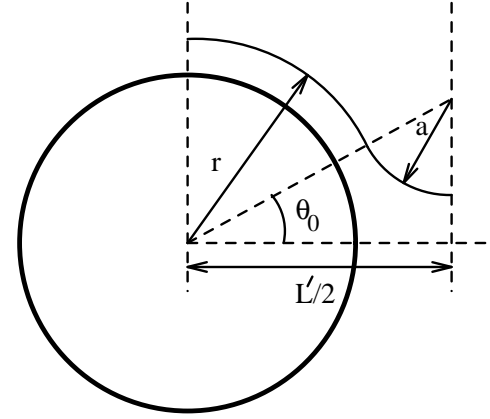


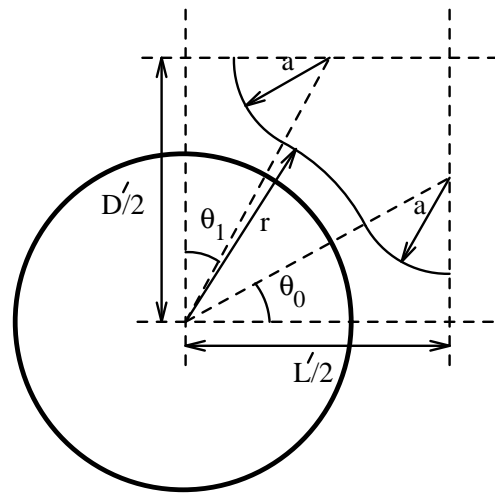
Figure 5



(i.)



(ii.)



(iii.)

Figure 6